JOURNAL OF APPLIED ELECTROCHEMISTRY 23 (1993) 615–624

Thermoanalytical investigation on the formation of IrO_2-based mixed oxide coatings*

J. KRISTÓF, J. LISZI

University of Veszprém, P.O. Box 158, H-8201 Veszprém, Hungary

P. SZABÓ

Research Laboratory for Inorganic Chemistry, Hungarian Academy of Sciences, P.O. Box 132, Budapest, Hungary

A. BARBIERI, A. DE BATTISTI

Centro C.N.R. per lo Studio della Fotochimica e Reattività S.E.C.C. and Dipartimento di Chimica dell'Università, via L Borsari, 46, I-44100 Ferrara, Italy

Received 7 July 1992; revised 16 November 1992

The formation reactions of IrO_2/TiO_2 mixed oxide films supported on titanium metal plate were followed by thermoanalytical (simultaneous TGA, DTG, DTA) and combined thermoanalytical-mass spectrometric (TGA-MS) techniques. The electrochemical characterization of the fired coatings was made by cyclic voltammetry. The thermal decomposition of the titanium precursor salt, titanium diisopropoxide bis-2,4-pentanedionate, shows a major change in the presence of hydrated iridium (III) chloride. Due to the catalytic effect of the added noble metal, an almost complete conversion of the organic components of the precursor mixture to CO_2 and H_2O is observed in the combustion stage. Chlorine, from thermal decomposition of the iridium salt, is produced in a separate stage at higher temperatures, indicating that a sequence of steps occurs prior to the oxide formation. For iridium chloride alone a complexation between the metal ion and the solvent (isopropanol) is observed, leading eventually to H_2O and CO_2 production (combustion step) between 300 and 500° C. The cyclic voltammetry results indicate that the features of the precursor reaction affect the charge storage capacity of the oxide films.

1. Introduction

The promising application of oxide electrodes in different branches of industrial electrochemistry, such as galvanics, waste water treatment, organic electrosynthesis and hydrogen evolution raise new questions about the optimal choice of components of the mixed oxide electrocalysts, and of the parameters of their preparation. Correlations between the composition of the materials and the results of their electrochemical characterization are an important step and several papers have appeared on the subject [1–6]. The role of the temperature at which the pyrolysis of precursor salts is carried out has also been studied, essentially for the case of one component systems [7–9]. The precursor path leading to the final oxide products is, however, quite complex even for the case of one-component systems (e.g. [10–13]). Its understanding requires information on the roles played by the nature and amount of precursor salts, and of the solvents used for their solution. These variables affect the microstructure and surface morphology of the mixed oxide electrodes and their electrochemical behaviour. While methods for the electrochemical characterization of oxide electrocatalysts are well established, the study of the mechanisms of their formation has been considered only in a limited number of papers [10–13].

In the present work the results of a detailed thermoanalytical study are reported on the formation of IrO_2/TiO_2 electrocatalysts by thermal decomposition of $IrCl_3.3H_2O$/titanium(diisopropoxide) bis-2,4-pentanedionate precursor mixtures differing in the Ir/Ti atom ratio. An electrochemical characterization of the samples has also been carried out by cyclic voltammetry and an interpretation of the results has been attempted on the basis of the thermoanalytical picture.

2. Experimental details

IrO_2/TiO_2 mixed oxide samples were prepared on titanium strips (size 4 mm × 12 mm, thickness 0.1 mm). Prior to deposition, the strips used as support were etched in 20% oxalic acid at a temperature of 80° C for 10 min, rinsed with distilled water and acetone, and finally dried at room temperature. The precursor

* This paper is dedicated to Professor Brian E. Conway on the occasion of his 65th birthday, and in recognition of his outstanding contribution to electrochemistry.

0021-891X

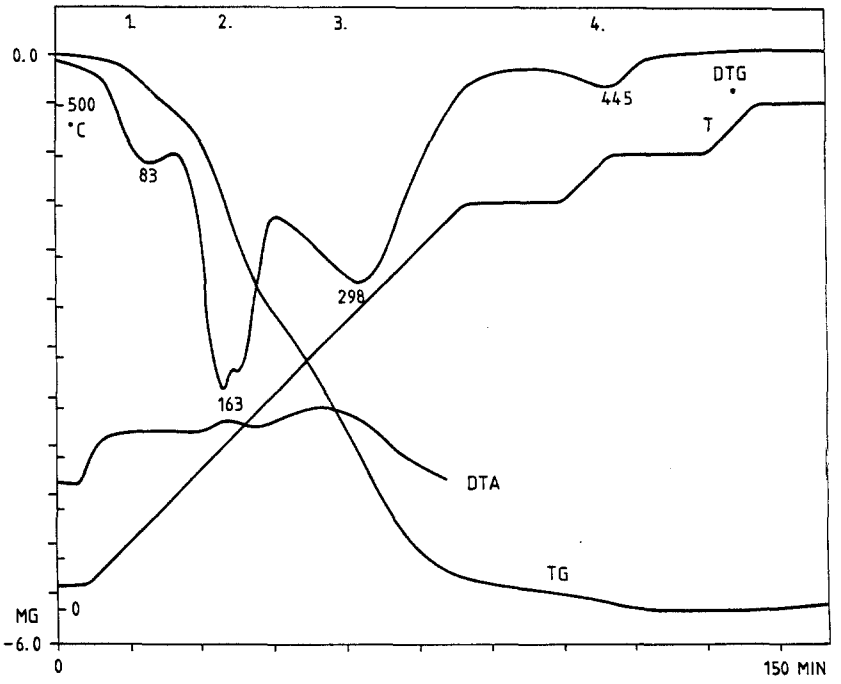

Fig. 1. Thermoanalytical curves of the coating 0%Ir–100%Ti.

salt mixtures were made of $IrCl_3.3H_2O$ (Ventron Gmbh) and titanium diisopropoxide bis-2,4-pentanedionate (Ventron Gmbh), hereinafter indicated as TIP. Equimolar isopropanolic stock solutions of the two components were prepared, and the solutions of the two precursor salts were made by mixing them in suitable ratios. To obtain observable mass and enthalpy changes in thermoanalytical investigations, higher mixed-salt loadings were needed. Solutions of the required composition were applied drop-by-drop onto the surface of the titanium strips and dried by hot air (about 60° C), layer-by-layer, until the total mass of the coating mixture reached 5 to 10 mg. For samples used in electrochemical investigation the preparation procedure was substantially similar [14].

Thermoanalytical investigations were carried out by means of a derivatograph (Hungarian Optical, C-type instrument). The experimental atmosphere was oxygen. The heating rate was 5° C min^{-1}. Isothermal stages at 400, 450, 500° C, with a duration of 20 min each, were included in the heating programme. Eight strips, coated following the above procedure, were placed side by side in a ceramic crucible. The furnace was purged with oxygen dried on P_2O_5, at a controlled flow rate of 15 dm^3h^{-1}. In order to reduce random noise and to compensate for the buoyancy effect, a baseline correction was made after each run

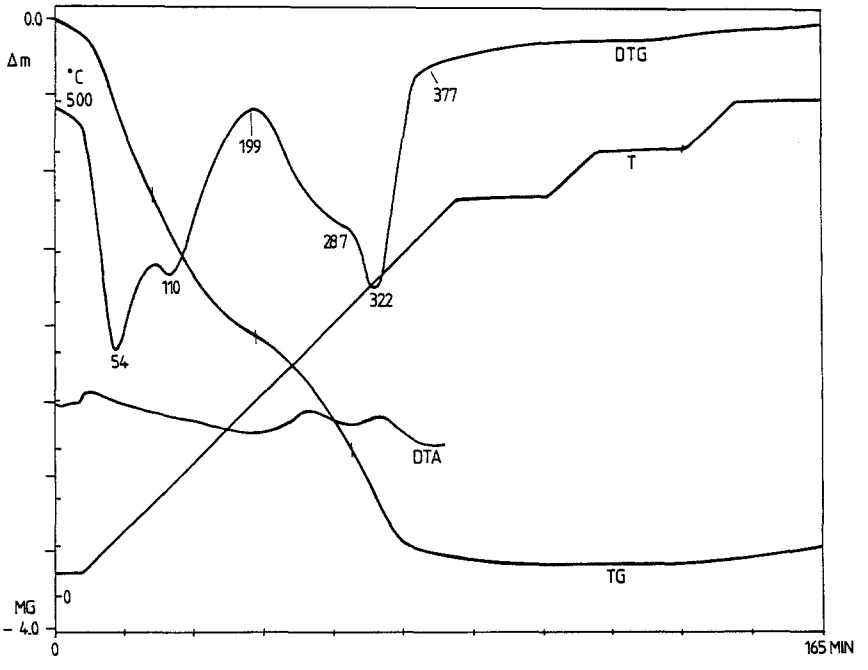

Fig. 2. Thermoanalytical curves of the coating 10%Ir–90%Ti.

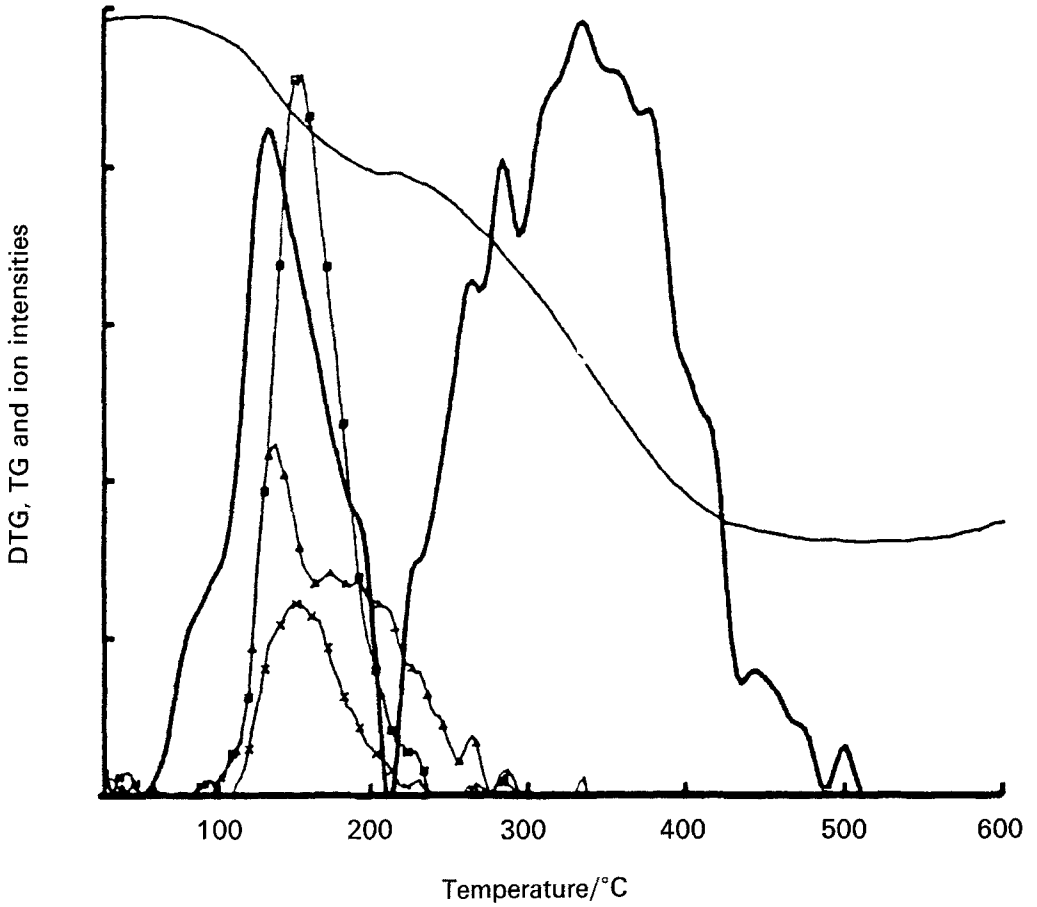

Fig. 3. TG, DTG and ion intensity curves of the coating 10%Ir–90%Ti. (□), m/z = 41; (△), m/z = 43; (×), m/z = 27; (– – –), TG; (——), DTG.

(the TGA curve was recorded using an empty crucible under identical experimental conditions and subtracted from the recorded curve, by computer). The four basic thermoanalytical curves for temperature (T), thermogravimetry (TGA), derivative thermogravimetry (DTG), and differential thermal analysis (DTA), were recorded simultaneously.

Combined thermogravimetric-mass spectrometric (TGA-MS) investigations were performed in a Perkin–Elmer TGS-2/System 4 thermobalance coupled with a Balzers MG 511-type mass spectrometer provided with a data acquisition and data processing unit. Electron impact ionization was made in a cross-beam ion source operated at 70 V. In this case coated Ti strips were cut into three pieces (4 × 4 mm size) and placed into a ceramic crucible. The mixed-salt loading amounted, in this case, to 2–3 mg. The coating heating rate was 10° C min^{-1}. The purge gas was a mixture of high purity argon and oxygen (30% oxygen). Part of the carrier gas mixed with the gaseous decomposition products formed, was introduced into the ion source of the mass spectrometer through a silica capillary. Mass spectrometric intensities up to m/z = 88 were measured as a function of temperature. Ion curves close to the noise level were disregarded. The mathematical criterion for rejection was a signal-to-noise ratio lower than 10.

Cyclic voltammetry experiments were carried out by a Solartron 1286 electrochemical interface, operated by dedicated software [15]. The electrodes were tested in 1 M $HClO_4$ (Fluka Purissimum). The polarization range was 0.00–1.20 V vs SCE, and potential scan rates between 0.010 and 0.300 V s^{-1} were chosen.

3. Results and discussion

3.1. *Thermoanalytical data*

The T, TGA, DTG and DTA curves for a 8.90 mg coating of TIP are shown in Fig. 1. As discussed previously [8], the mass loss step at 83° C is due to the absorbed solvent removal, while the combustion of the organic complex takes place at 163 and 298° C. At 445° C the burning of elemental carbon obtained in the combustion process occurs.

The thermoanalytical curves of the coating containing 10 mol % of Ir and 90 mol % of Ti (10%Ir–90%Ti) are shown in Fig. 2. As a result of the addition of hydrated iridium (III) chloride a significant change in the thermolysis pattern can be observed. The step at 445° C completely disappears and the two exothermic peaks in the DTA curve indicate a two-stage combustion process in the 200–380° C temperature range. The iridium compound apparently has a definite catalytic effect on the combustion process. The mass spectrometric results obtained for the same precursor mixture are shown in Figs 3 and 4. The DTG peak observed at 54° C in Fig. 2, is absent in Fig. 4. Considering that the only difference between the two experiments is sample conditioning, with dry O_2/Ar mixture, for the

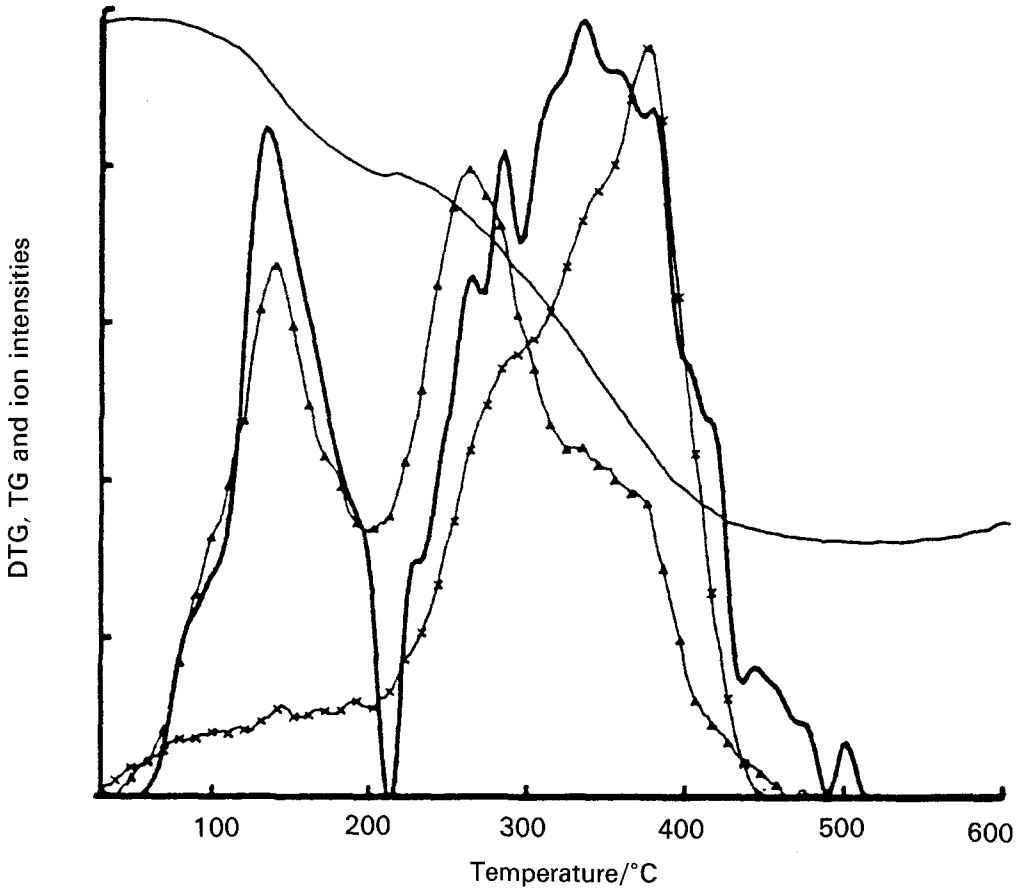

Fig. 4. TG, DTG and ion intensity curves of the coating 10%Ir–90%Ti. (△), m/z = 18; (×), m/z = 44.

sample for TGA-MS test, this peak could then be ascribed to solvent (isopropanol) removal. The peak shoulder at 100° C is due to liberation of crystallization water. In Fig. 3, ion intensity curves for fragments C_3H_5 (or C_2HO), C_2H_3O (or C_3H_7), and C_2H_3 (mass numbers 41, 43, 27, respectively), show that in the range 100–200° C, the dominant process is the formation of organic crack products. The cracking process slightly overlaps with the combustion stage, but it goes to virtual completion by 250° C. In the combustion stage (220–430° C in Fig. 4) water (m/z = 18) and carbon dioxide (m/z = 44) are formed. Again, the almost complete conversion of residual organic substances in the sample, to carbon dioxide

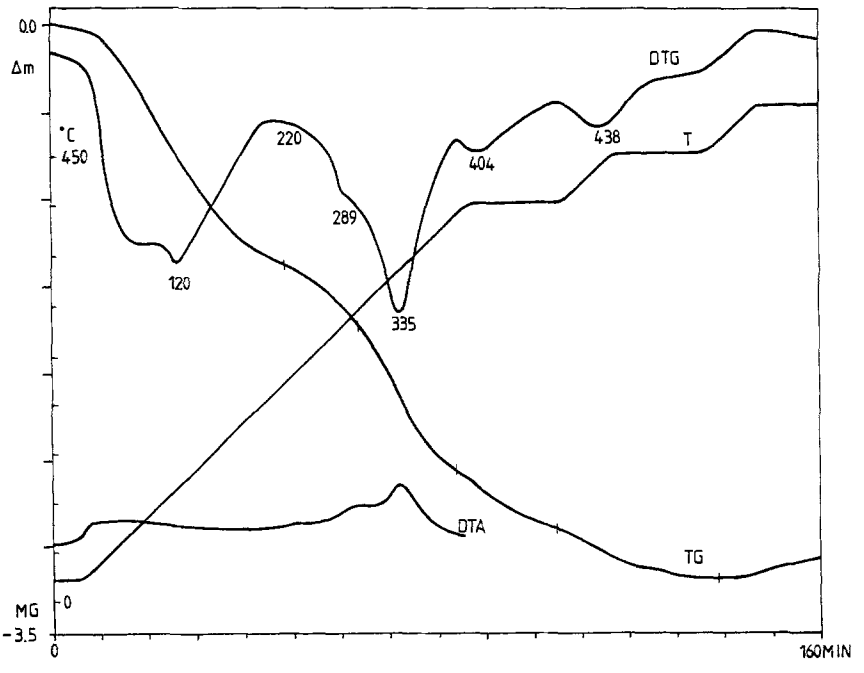

Fig. 5. Thermoanalytical curves of the coating 50%Ir–50%Ti.

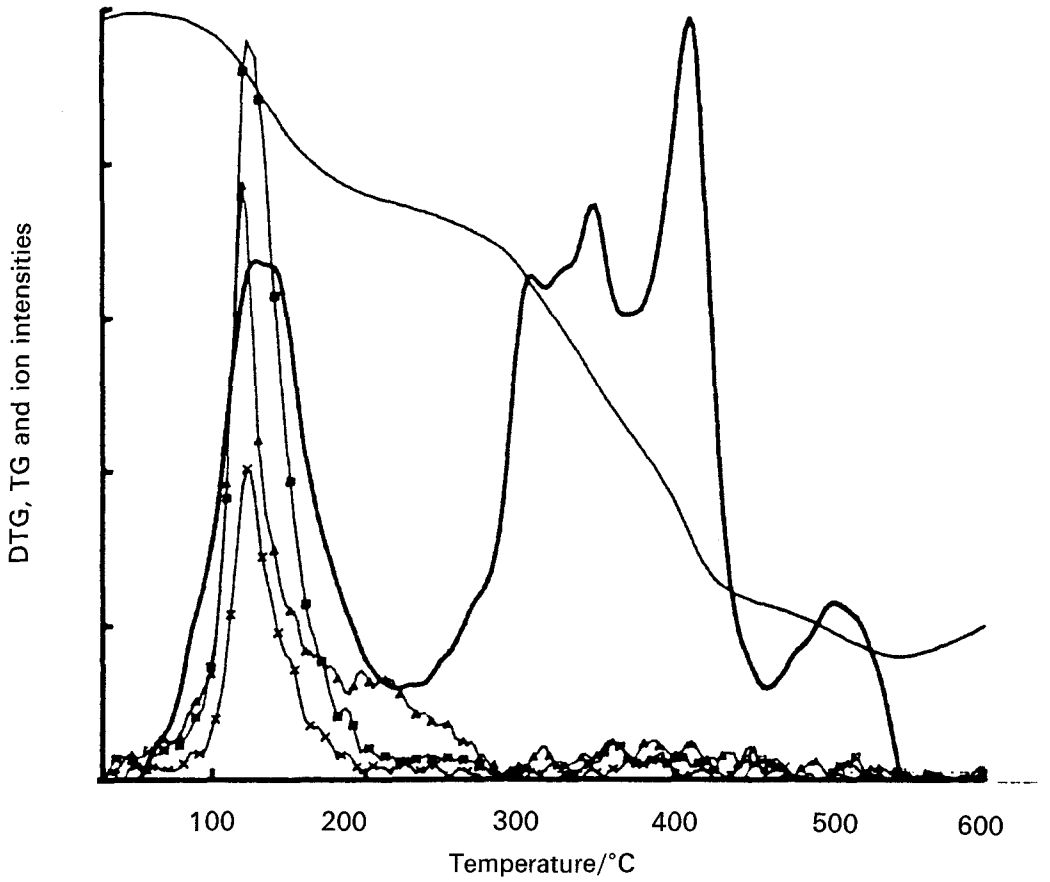

Fig. 6. TG, DTG and ion intensity curves of the coating 50%Ir–50%Ti. (□), m/z = 41; (△), m/z = 43; (×), m/z = 42; (– – –), TG; (——), DTG.

and water can only be explained by the catalytic effect of the iridium salt. It is interesting to note that the ion intensity curves of H_2O and CO_2 show a 'mirror image' pattern. This may be taken as an indication of the fact that at the beginning of the combustion process water elimination is dominant, while towards the end of the process carbon dioxide production prevails. Above 430° C a small decomposition step is recognized. This is associated with the formation of chlorine. It can therefore be concluded that the thermal decomposition of iridium(III) chloride takes place at the high temperature end of the overall decomposition process.

The thermoanalytical results relative to the coating containing 50 mol % of iridium and 50 mol % of titanium are shown in Fig. 5. Here the decomposition process can be divided into three main stages. From ambient temperature to 220° C, solvent, crystallization water and organic crack products are formed. In the 220–390° C range, a combustion process takes place, as indicated by the exothermic peaks in the DTA curve, at 289° C and 335° C. Above 390° C a significant mass loss is observed, which is probably related to chlorine elimination from the coating. The mass spectrometric results obtained for this coating composition are given in Figs 6 and 7. As already found for ion intensity curves in Fig. 3 for the 10%Ir–90%Ti composition, formation of crack products takes place in the temperature range 20–220° C. Fragments C_3H_5 (or C_2HO), C_2H_3O (or C_3H_7) and C_3H_6 (or C_2H_2O), whose mass numbers are 41, 43, 42, respectively, seem to be the main products. Data in Fig. 7 show that in the combustion process only water and carbon dioxide are formed. The almost complete combustion of organics in two-component precursor mixtures is therefore confirmed. Above 450° C a separate decomposition stage is observed, which can be attributed to the chlorine elimination, as a result of the conversion of iridium chloride to iridium oxide.

The T, TGA, DTG, DTA curves of the coating obtained from isopropanolic solutions of hydrated iridium(III) chloride are shown in Fig. 8. In this case the mass loss step in the range 20–260° C is expected to be associated with the release of residual solvent and crystallization water. The mass loss step at 369° C amounts to about 7% of the total mass of iridium chloride coating and cannot be readily interpreted on the basis of the thermoanalytical curves only. The thermal decomposition steps at higher temperatures (453 and 494 °C) are associated with the decomposition of iridium chloride. In order to find further information on the decomposition mechanism, TGA-MS investigations were also made. Results are reported in Figs 9 and 10. The ion intensity curves indicate the formation of organic crack products, e.g. C_3H_5 (or C_2HO), C_2H_2O (or C_3H_6), and C_2H_3O. The respective mass numbers have been previously reported. Release of CO_2 and H_2O is also observed. Somewhat surprisingly, a combustion step, witnessed by the shape of H_2O (m/z = 18) and CO_2 (m/z = 44) ion

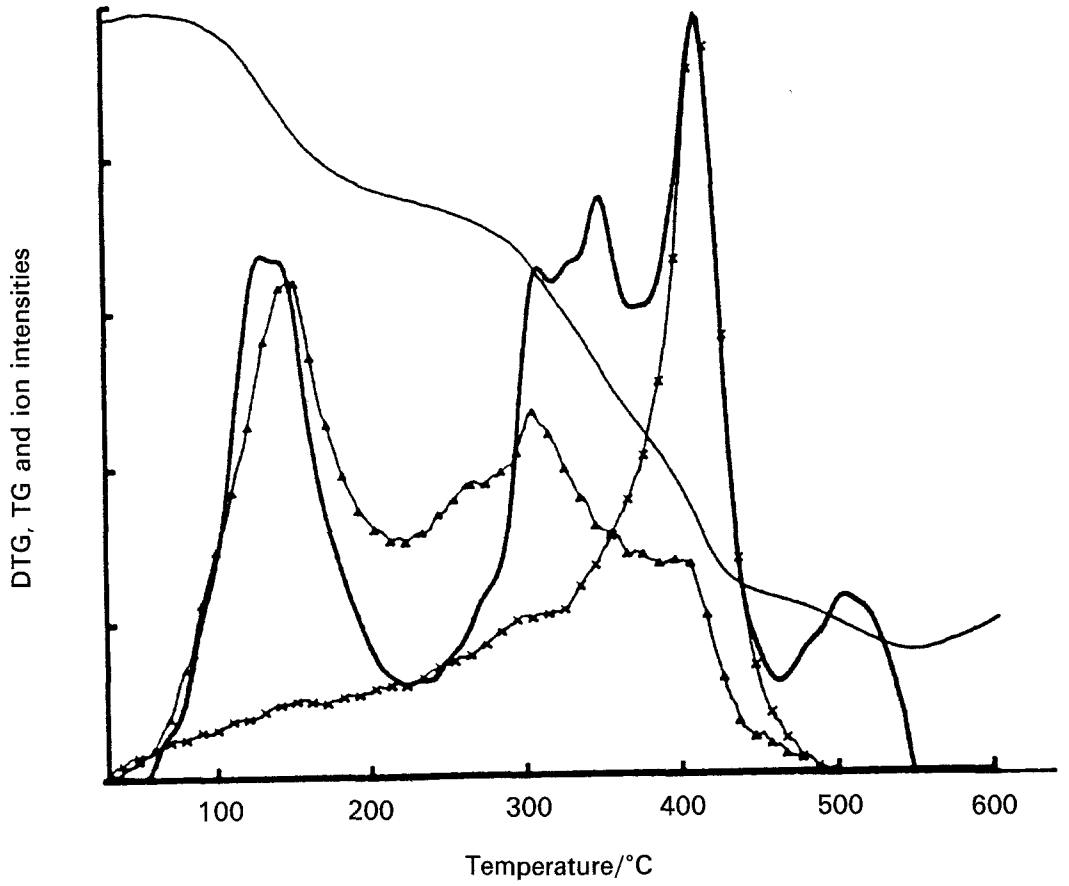

Fig. 7. TG, DTG and ion intensity curves of the coating 50%Ir–50%Ti. (△), m/z = 18; (×), m/z = 44; (– – –), TG; (——), DTG.

intensity curves, still exists in the 260–500° C temperature range. In this case no titanium complex is present in the coating, and the boiling point of the solvent is low. TGA-MS patterns in Fig. 10 can then be tentatively explained by a partial substitution of crystallization water in the iridium salt, by isopropanol molecules. The thermal decomposition of this complex takes place at high temperatures. The structural identification of the complex, and the mechanism of its formation and pyrolysis, require further investigation. The mass loss step above 450° C is due to chlorine release, as discussed in the previous cases.

As a general observation, small additions of iridium

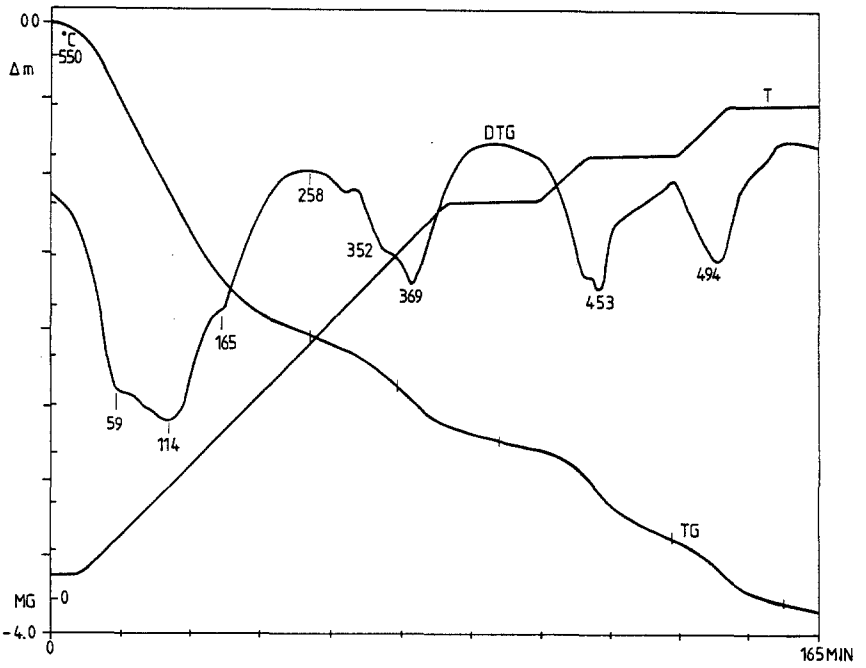

Fig. 8. Thermoanalytical curves of the coating 100%Ir–0%Ti.

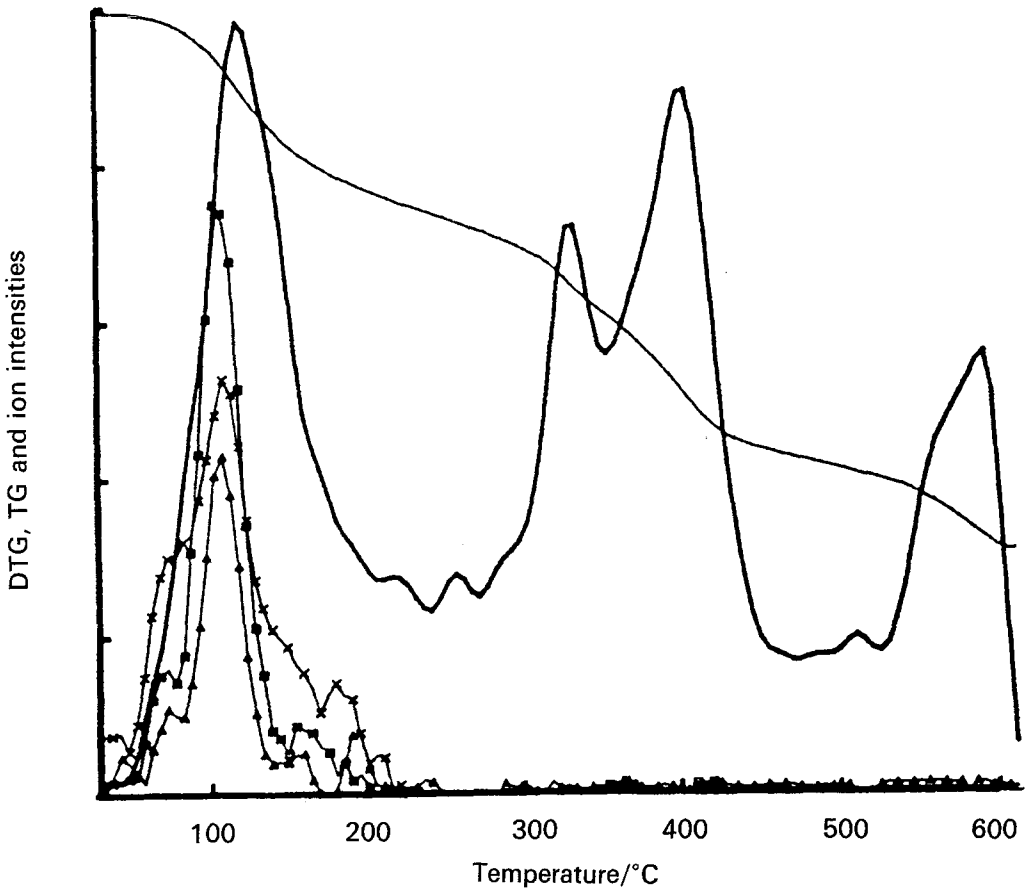

Fig. 9. TG, DTG and ion intensity curves of the coating 100%Ir–0%Ti; (□), m/z = 41; (△), m/z = 42; (×), m/z = 43; (- - -), TG; (——), DTG.

salt to the titanium complex cause a decrease in the temperature at which the combustion of organic species in the precursor salt films occurs at a maximum rate. A further increase of the iridium mol fraction, slightly shifts this temperature towards higher values. This effect is shown in Fig. 11. The temperature at which chlorine release, i.e. the conversion of iridium chloride into iridium oxide, takes place at the highest rate, also increases with increasing iridium content in the precursor mixture. The correlation between the temperature of maximum rate of chlorine release and the iridium concentration in the precursor mixture, is shown in Fig. 12. Due to the shift of the two main thermolytic processes to lower temperatures, the bond rearrangements and migration of components in the residual solid are more difficult. An analogous indication is found in the preparation of IrO_2 films by reactive sputtering [16]. In this case, samples grown at lower temperatures show a practically amorphous microstructure and low conductivity. Only annealing at higher temperatures allows the achievement of a well defined rutile structure with the expected conductivity values.

Thus, additions of iridium chloride to the precursor salt mixture, at levels of 10–50 mol % would then allow the formation of more porous and defective mixed-oxide films. The chloride thermolysis, in particular, decreases from about 600 to 400° C changing the iridium chloride concentration from 100% to 10%. The effect of the film composition on its microstructure is therefore expected to be significant.

3.2. *Characterization of the electrode materials by cyclic voltammetry*

Typical voltammograms, obtained at different potential scan rates, for an electrode containing 50 mol % of IrO_2, are shown in Fig. 13. A single pair of peaks, due to the Ir(IV)/Ir(III) redox couple [17, 18] occurs. Similar features are also observed in the case of other electrode compositions studied, with the exception of pure IrO_2 films, whose voltammograms do not exhibit well defined peaks. Large background currents which, at least in first approach, can be assigned a capacitive nature are also observed in any case. On the basis of cyclic voltammetry results, peak charges can be calculated and related, according to the above assumption, to the number of electroactive sites at the electrode surface. In Fig. 14, anodic peak charges, Q, have been plotted as a function of the nominal iridium concentration in the electrodes. Results obtained in the range of potential scan rates between 0.002 and 0.100 V s^{-1} have also been reported. Peak charges increase with decreasing potential scan rate. This effect is quite significant for the two electrodes containing 20 and 30 mol % of iridium, which also exhibit maximum values of peak charge Q. From results in Fig. 14, numbers of electroactive sites per apparent square centimetre as high as (2–3) × 10^{16} are found,

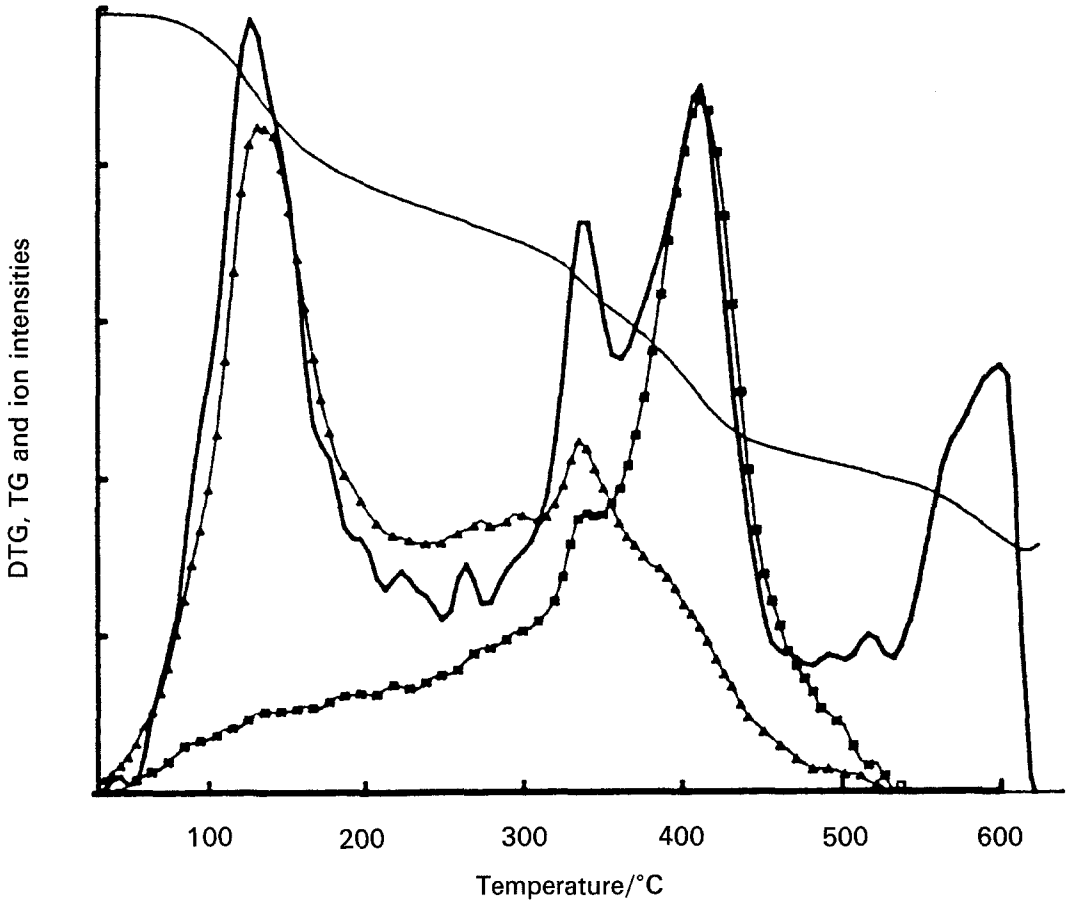

Fig. 10. TG, DTG and ion intensity curves of the coating 100%Ir–0%Ti. (△), m/z = 18; (×), m/z = 44; (– – –), TG; (——), DTG.

under the most favourable conditions of electrode composition and potential scan rate. The lower analytical concentration of noble metal in the 20 and 30 mol % samples, compared with those containing 70 and 80 mol %, must be compensated by some other effect. Significant roles may be played by surface segregation phenomena and/or surface morphology. Both can control the total number of electroactive sites which effectively take part in redox processes at this type of oxide electrode. Both can be affected, in turn, by the preparation parameters. As far as segregation phenomena are concerned, depth profiling results on IrO_2/TiO_2 [19] and RuO_2/TiO_2 [20] electrodes have shown that the concentration of metal ion species in the near surface region is only slightly affected by changes of their nominal bulk composition, due to a local enrichment with titanium oxide species. This indicates that the changes in nominal bulk composition of electrode films of this type are somewhat buffered by the segregation of titanium oxide species in the surface region. Indirect information on porosity of the film electrodes can be obtained from thermoanalytical results. The rate of conversion to the oxide mixture is larger, and the temperature at which it takes place, is lower, for the oxide mixtures with intermediate IrO_2 concentrations. In this composition

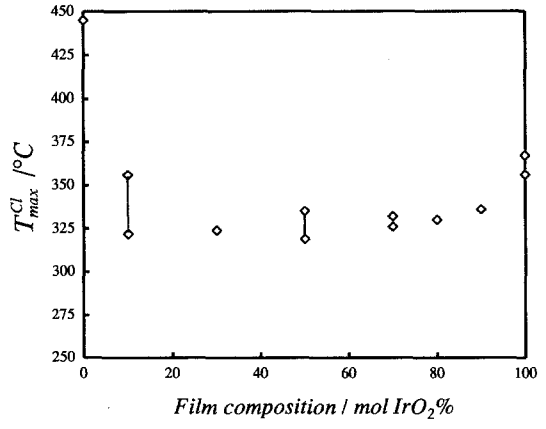

Fig. 11. Dependence of the maximum combustion rate temperature, T_{max}, on the coating composition.

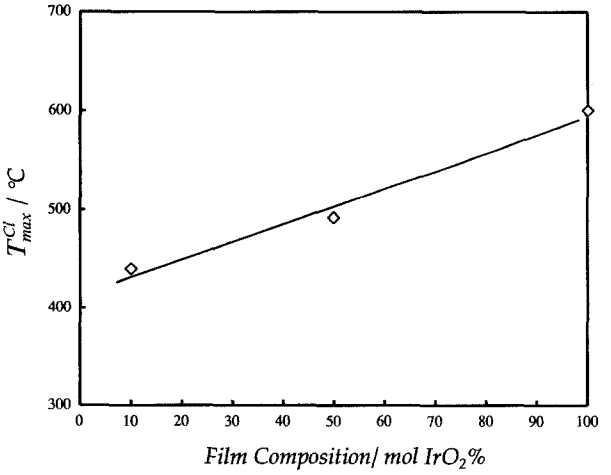

Fig. 12. Dependence of the maximum chlorine release rate temperature T^{Cl}_{max}, on the coating composition.

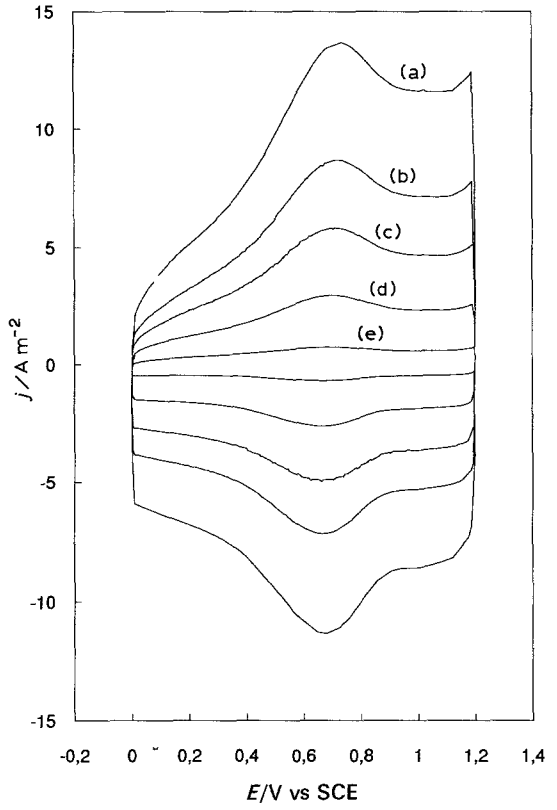

Fig. 13. Cyclic voltammograms at different potential scan rates, for a IrO_2/TiO_2 electrode immersed in 1 M $HClO_4$. Coating composition: 50 mol % IrO_2. Scan rate/V s^{-1}: (a) 0.080, (b) 0.050, (c) 0.030, (d) 0.010 and (e) 0.002.

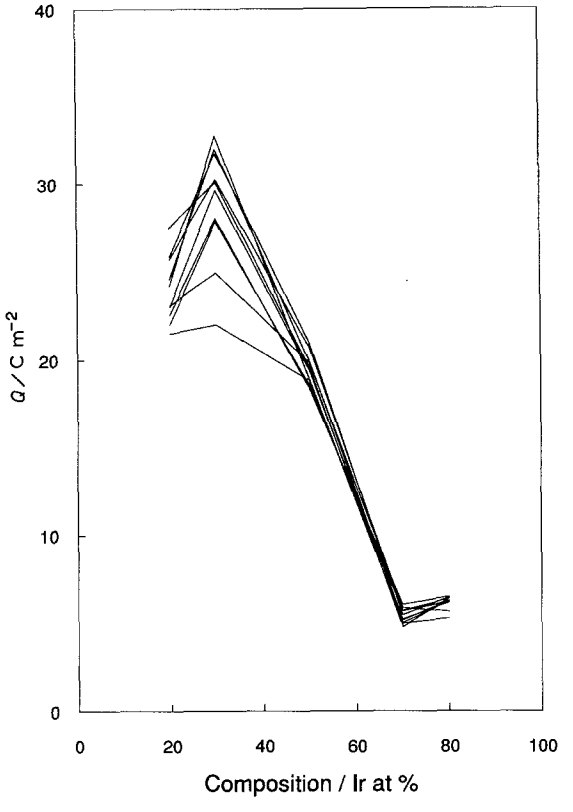

Fig. 14. Anodic peak charge, Q, against nominal average composition of the electrodes, at different potential scan rates, between 0.00 and 0.100 V s^{-1}. Solution: 1 N $HClO_4$.

range, the electrode films retain more of the gel-like structure typical of the precursor salt precipitate formed during the evaporation of solvents prior to thermal treatment. The large number of electroactive sites in Fig. 14 imply rather large roughness factors, of the order of about 300. The dependence of peak charge on potential scan rate for the two samples with lowest noble metal concentration are not easily explained, if the films are imagined to consist of rutile structured crystallites separated by a small number of atomic layers. Microstructural data on IrO_2 [21], and stoichiometry results obtained by RBS [22] suggest that, even in the simplest case of a one-component film, crystallites are separated by large amorphous or microcrystalline regions where chemical and microstructural defects are collected. These regions are a consequence of the incomplete transformation of precipitated precursor salts and are likely to maintain the gel features of the latter. According to thermoanalytical results the addition of a second component favours this 'memory effect' and an enhancement of the role of the noncrystalline part of the films. This expectation is confirmed by X-ray diffractometric data [23]. The above considerations support the idea that in the near-surface region of thermally prepared IrO_2/TiO_2 film electrodes, the number of electroactive iridium ions, is essentially controlled by the roughness factor. This can also acount for results in Fig. 14.

4. Conclusions

The thermoanalytical investigation of the formation of IrO_2/TiO_2 mixed-oxide coatings supplies useful information on the nature of the chemical reactions taking place in the preparation process. Considering the thermolysis of the iridium (III) hydrated chloride–titanium diisopropoxide bis-2,4-pentanedionate precursor system, on the basis of TGA, DTG, DTA and TGA-MS data, three main temperature regions can be distinguished. Between ambient temperature and 220° C, solvent and crystallization water are released, together with organic cracking products. Between 220 and 400–450° C, combustion of residual organic substances in the films takes place. The thermal decomposition of iridium chloride to dioxide, accompanied by chlorine liberation, occurs above 400° C.

The combustion steps, as with chlorine release, occur at higher rates and lower temperatures in film compositions between 20 and 50 mol % of iridium oxide. These features of the precursor path are responsible for the larger microstructural defectivity and the greater roughness factor of film electrodes with compositions included in the mentioned range. Cyclic voltammetry data on voltammetric peak charges and the related number of electroactive sites in the films are in agreement with the predictions formulated on the basis of thermoanalytical results. The tools of thermoanalysis are quite powerful in the description of changes taking place in the precursor salt thermolysis, allowing, in principle, a rationalization of the choice

of the electrocatalyst composition, and of the parameters of the precursor path.

References

[1] S. Trasatti and G. Lodi, in 'Electrodes of Conductive Metal Oxides', Part B, (edited by S. Trasatti), Elsevier, Amsterdam (1981) pp. 521–626.

[2] L. D. Burke and O. J. Murphy, *J. Electroanal. Chem.* **112** (1980) 39.

[3] C. Angelinetta, S. Trasatti, Lj. D. Atanasoska and R. T. Atanasoski, *ibid.* **214** (1986) 535.

[4] L. D. Murphy and M. McCarthy, *Electrochimica Acta* **29** (1984) 211.

[5] J. F. C. Boots and S. Trasatti, *J. Electrochem. Soc.* **137** (1990) 3784.

[6] B. E. Conway, Gu Ping, A. De Battisti, A. Barbieri and G. Battaglin, *J. Mater. Chem.* **1** (1991) 725.

[7] G. Lodi, E. Sivieri, A. De Battisti and S. Trasatti, *J. Appl. Electrochem.* **8** (1978) 135.

[8] S. Ardizzone, M. Falciola and S. Trasatti, *J. Electrochem. Soc.* **136** (1989) 1545.

[9] G. W. Jang, E. W. Tsai and K. Rajeshwar, *J. Electroanal. Chem.* **263** (1989) 383.

[10] A. E. Newkirk and D. W. McKee, *J. Catal* **11** (1968) 370.

[11] G. W. Jang and K. Rajeshwar, *J. Electrochem. Soc.* **134** (1987) 1830.

[12] G. Lodi, A. De Battisti, A. Benedetti, G. Fagherazzi and J. Kristof, *J. Electroanal. Chem.* **256** (1988) 441.

[13] G. Lodi, A. De Battisti, G. Bordin, C. De Asmundis, A. Benedetti, *J. Electroanal. Chem.* **277** (1990) 139.

[14] G. Lodi, C. Bighi, C. De Asmundis, *Mater. Chem.* **1** (1976) 177.

[15] A. Barbieri, R. Cenacchi, Unpublished results, Università Ferrara, 1988.

[16] S. Hackwood, A. H. Dayem, G. Beni, *Phys. Rev. B* **26** (1982) 471.

[17] S. Ardizzone, A. Carugati and S. Trasatti, *J. Electroanal. Chem.* **126** (1981) 287.

[18] P. G. Pickup and V. Birss, *ibid.* **240** (1988) 185.

[19] A. De Battisti, A. Barbieri, A. Giatti, G. Battaglin, S. Daolio, A. Boscolo Boscoletto, *J. Mater. Chem.* **1** (1991) 191.

[20] A. De Battisti, G. Lodi, M. Cappadonia, G. Battaglin and R. Kötz, *J. Electrochem. Soc.* **136** (1989) 2596.

[21] A. Benedetti, S. Polizzi, P. Riello, A. De Battisti, A. Maldotti, *J. Mater. Chem.* **1** (1991) 511.

[22] G. Battaglin, A. Carnera, G. Della Mea, G. Lodi and S. Trasatti, *J. Chem. Soc., Faraday Trans. I* **81** (1985) 2995.

[23] A. De Battisti and A. Barbieri, University of Ferrara, unpublished results (1991).